ANL/ET/CP--84554
CONF-950740--88

VIBRATION AND STABILITY OF TWO TUBES IN CROSSFLOW*

S. Zhu and S. S. Chen
Energy Technology Division
Argonne National Laboratory
Argonne, Illinois

Submitted for presentation at the ASME/JSME PVP Conference, July 23-27, 1995, Honolulu, Hawaii.

*This work was jointly funded by the U. S. Department of Energy, Office of Basic Energy Sciences, Division of Engineering and Geosciences, under Contract W-31-109-Eng-38, and by Taiwan Power Company under an agreement with the U. S. Department of Energy, Contract Agreement 31-109-Eng-38-85847.

ABSTRACT

Two tubes in tandem and normal to flow are studied on the basis of the unsteady flow theory. Motion-dependent fluid forces are measured in a water channel for the pitch-to-diameter ratio of 1.35. From the measured fluid forces, fluid damping and stiffness are calculated as a function of reduced flow velocity and several Reynolds numbers. Once fluid-damping and fluid-stiffness coefficients are known, coupled vibration and stability of two tubes in crossflow can be predicted.

1. INTRODUCTION

Flow-induced vibration of two tubes in crossflow has been studied extensively. It includes vibration in stationary fluid, turbulent buffeting, vortex-induced vibration, and wake induced flutter. Several reviews were published by Chen (1986) and Zdravkovich (1977).

The flow field around two tubes is very complex. It depends on Reynolds number and tube arrangement, as well as on incoming flow conditions. The interaction of fluid flow with tube oscillation is even more complicated. Various approximate theories have been developed to describe the tube response in crossflow. At this time, it remains difficult to predict the response of the two tubes because the fluid forces acting on the tubes and the motion-dependent fluid forces cannot be calculated with confidence.

On the basis of the available information, the general characteristics of tube response in crossflow are not well understood in the various parameter ranges, since most of the experimental data were obtained for specific applications. A systematic study is needed to quantify the response of two tubes under different flow conditions. The objective of this paper is to present an unsteady flow theory for two tubes normal to the flow, or two tubes in tandem, with a pitch-to-diameter ratio of 1.35 (see Fig. 1, where D is tube diameter).

For two tubes oscillating in crossflow, the fluid forces acting on the tubes are f_i and g_i ($i = 1,2$) in the x and y directions. The corresponding tube displacement components of the tubes are u_i and v_i. The fluid forces acting on the tube due to the tube motion are given by (Chen 1987)

$$f_j = -\rho\pi R^2 \sum_{k=1}^{2}\left(\alpha_{jk}\frac{\partial^2 u_k}{\partial t^2} + \sigma_{jk}\frac{\partial^2 v_k}{\partial t^2}\right) + \frac{\rho U^2}{\omega}\sum_{j=1}^{2}\left(\alpha'_{jk}\frac{\partial u_k}{\partial t} + \sigma'_{jk}\frac{\partial v_k}{\partial t}\right)$$

$$+\rho U^2 \sum_{j=1}^{2}\left(\alpha''_{jk}u_k + \sigma''_{jk}v_k\right) \tag{1}$$

and

$$g_j = -\rho\pi R^2 \sum_{k=1}^{2}\left(\tau_{jk}\frac{\partial^2 u_k}{\partial t^2} + \beta_{jk}\frac{\partial^2 v_k}{\partial t^2}\right) + \frac{\rho U^2}{\omega}\sum_{k=1}^{2}\left(\tau'_{jk}\frac{\partial u_k}{\partial t} + \beta'_{jk}\frac{\partial v_k}{\partial t}\right)$$

$$+\rho U^2 \sum_{j=1}^{2}\left(\tau''_{jk}u_k + \beta''_{jk}v_k\right) \quad , \tag{2}$$

where ρ is fluid density; R is tube radius; t is time; ω is circular frequency of tube oscillations; U is flow velocity, α_{jk}, β_{jk}, σ_{jk}, and τ_{jk} are added mass coefficients; α'_{jk}, β'_{jk}, σ'_{jk}, and τ'_{jk} are fluid damping coefficients; and α''_{jk}, β''_{jk}, σ''_{jk}, and τ''_{jk} are fluid-stiffness coefficients. The main purpose of this study is to measure the motion-dependent fluid-force coefficients for two tubes in crossflow. Once these fluid-force coefficients are obtained, tube response in various conditions can be analyzed on the basis of the unsteady flow theory.

2. EXPERIMENTAL SET-UP

The two tubes tested are shown in Fig. 1, where the tubes are normal to flow (Fig. 1a) or in tandem (Fig. 1b). A water channel, 18 in. wide and 15 in. deep, is used. Water is pumped into an input tank and then passes through a series of screens and honeycombs and finally into the rectangular channel. The water level is controlled by standpipes in the output tank and the flow is controlled by the running speed of the pump motor.

Flow velocity is measured with a current flow meter. The rate of propeller rotation is directly proportional to stream velocity and therefore the sensor output signal is not effected by other factors, such as water conductivity, temperature, and suspended particulates.

Tubes are supported by flexible tubes attached to the stainless steel tubes with a 2.54-cm OD, a 0.071-cm wall thickness, and a 38.1-cm length. Two sets of strain gauges are placed on the outer surface of the smaller tube where the outer surface of the tube has been machined to give an octagonal cross section (Chen, Zhu, and Jendrzejczyk 1994). The natural frequencies of the tubes are as follows:

Tube No.	Total Mass (g)	Natural Frequencies (Hz)	
		x Direction	Y Direction
1	194	9.9	11.6
2	198	10.3	10.3

The force transducers are calibrated by the dynamic method. The tube is connected to an exciter and is excited at a given frequency and amplitude in air or water. Then, the inertia forces due to the sinusoidal oscillations are used to determine the calibration constant.

3. COUPLED VIBRATION IN STATIONARY FLUID

When two tubes are placed at a pitch-to-diameter of 1.35 in water, fluid coupling can be significant. The fluid coupling effect can be accounted for using the added mass matrices (Chen 1975). The added mass was calculated from potential flow theory and experiments were performed to confirm the theoretical results from the indirect measurement method of the effect of natural frequencies for tubes submerged in fluid (Chen and Jendrzejczyk 1978).

In this study, a direct method is used to quantify the effect of fluid coupling. In stationary fluid, U = 0; Eqs. 1 and 2 can be written as

$$f_j = -\rho\pi R^2 \sum_{k=1}^{2}\left(\alpha_{jk}\frac{\partial^2 u_k}{\partial t^2} + \sigma_{jk}\frac{\partial^2 v_k}{\partial t^2}\right)$$

$$+\rho\pi R^2\omega \sum_{k=1}^{2}\left(\overline{\alpha}'_{jk}\frac{\partial u_k}{\partial t} + \overline{\sigma}'_{jk}\frac{\partial v_k}{\partial t}\right), \qquad (3)$$

$$g_j = -\rho\pi R^2 \sum_{k=1}^{2}\left(\tau_{jk}\frac{\partial^2 u_k}{\partial t^2} + \beta_{jk}\frac{\partial^2 v_k}{\partial t^2}\right)$$

$$+\rho\pi R^2\omega \sum_{k=1}^{2}\left(\overline{\tau}'_{jk}\frac{\partial u_k}{\partial t} + \overline{\beta}'_{jk}\frac{\partial v_k}{\partial t}\right). \qquad (4)$$

The theoretical values of the added mass coefficients for two tubes normal to flow with pitch-to-diameter ratio of 1.35 are given as follows:

$$\begin{bmatrix}\alpha_{11} & \alpha_{12}\\ \alpha_{21} & \alpha_{22}\end{bmatrix} = \begin{bmatrix}1.0526 & -0.2845\\ -0.2845 & 1.0526\end{bmatrix}$$

$$\begin{bmatrix}\beta_{11} & \beta_{12}\\ \beta_{21} & \beta_{22}\end{bmatrix}=\begin{bmatrix}1.0526 & 0.2845\\ 0.2845 & 1.0526\end{bmatrix} \tag{5}$$

$$\tau_{jk} = \sigma_{jk} = 0, \quad j,k = 1,2.$$

In stationary fluid, added mass can be measured by measuring the forces acting on the tubes due to a sinusoidal excitation. Figures 2a-2d show force components, f_i and g_i due to the excitation of u_1 (Fig. 2e). It is noted that f_1 and g_2 are approximately in-phase with u_1 while f_2 and g_1 are approximately out-of-phase with u_1. From the time histories, and Eqs. 3 and 4, the added mass coefficients, α_{jk}, β_{jk}, σ_{jk}, and τ_{jk}, and damping coefficients, $\overline{\alpha}'_{jk}$, $\overline{\beta}'_{jk}$, $\overline{\sigma}'_{jk}$, and $\overline{\tau}'_{jk}$, can be calculated. Figure 3 shows the experimental data of the added mass and fluid-damping coefficients as a function of excitation amplitude at three frequencies. The measured added mass coefficients, α_{11} and α_{21}, agree well with the analytical solution. Fluid-damping coefficients in stationary fluid are small. In this case, σ_{jk} and τ_{jk} are zero theoretically and approximately zero experimentally. This direct measurement method can be used to measure added mass and fluid damping efficiently.

4. MOTION-DEPENDENT FLUID FORCES

The unsteady flow theory is used in this study. If tube 1 is excited in the x direction, its displacement is given by

$$u_1 = u \cos \omega t. \tag{6}$$

The fluid force acing on the two tubes can be written

$$
\begin{aligned}
f_1 &= \frac{1}{2}\rho U^2 c_{11} u \cos(\omega t + \phi_{11}), \\
f_2 &= \frac{1}{2}\rho U^2 c_{21} u \cos(\omega t + \phi_{21}), \\
g_1 &= \frac{1}{2}\rho U^2 d_{11} u \cos(\omega t + \psi_{11}), \\
g_2 &= \frac{1}{2}\rho U^2 d_{21} u \cos(\omega t + \psi_{21}),
\end{aligned}
\tag{7}
$$

where c_{11}, c_{21}, d_{11}, and d_{21} are coefficients and ϕ_{11}, ϕ_{21}, ψ_{11}, and ψ_{21} are phase angles. From Eqs. 1, 2, and 7, we can also write the fluid-force components as

$$
\begin{aligned}
f_1 &= \left(\rho\pi R^2\omega^2\alpha_{11} + \rho U^2\alpha''_{11}\right)u\cos\omega t - \rho U^2\alpha'_{11}u\sin\omega t, \\
f_2 &= \left(\rho\pi R^2\omega^2\alpha_{21} + \rho U^2\alpha''_{21}\right)u\cos\omega t - \rho U^2\alpha'_{21}u\sin\omega t, \\
g_1 &= \left(\rho\pi R^2\omega^2\tau_{11} + \rho U^2\tau''_{11}\right)u\cos\omega t - \rho U^2\tau'_{11}u\sin\omega t, \\
g_2 &= \left(\rho\pi R^2\omega^2\tau_{21} + \rho U^2\tau''_{21}\right)u\cos\omega t - \rho U^2\tau'_{21}u\sin\omega t.
\end{aligned}
\tag{8}
$$

Comparing Eqs. 7 and 8 yields

$$
\alpha''_{11} = \frac{1}{2}c_{11}\cos\phi_{11} - \frac{\pi^3}{U_r^2}\alpha_{11},
$$

$$\alpha_{21}'' = \frac{1}{2} c_{21} \cos\phi_{21} - \frac{\pi^3}{U_r^2} \alpha_{21},$$

$$\tau_{11}'' = \frac{1}{2} d_{11} \cos\psi_{11} - \frac{\pi^3}{U_r^2} \tau_{11}, \tag{9}$$

$$\tau_{21}'' = \frac{1}{2} d_{21} \cos\psi_{21} - \frac{\pi^3}{U_r^2} \tau_{21},$$

and

$$\alpha_{11}' = \frac{1}{2} c_{11} \sin\phi_{11},$$

$$\alpha_{21}' = \frac{1}{2} c_{21} \sin\phi_{21},$$

$$\tau_{11}' = \frac{1}{2} d_{11} \sin\psi_{11}, \tag{10}$$

$$\tau_{21}' = \frac{1}{2} d_{21} \sin\psi_{21}.$$

Other fluid-force coefficients can be measured by exciting tube 1 in the y direction and tube 2 in the x and y directions.

The following tests have been performed:

- Two tubes normal to flow (Fig. 1a): Tube 1 was excited in the x and y directions.

- Two tubes in tandem (Fig. 1b): The upstream tube, tube 1, and the downstream tube, tube 2, are excited in the x and y directions.

In each test, the excitation frequency varies from 0.1 to 2.3 Hz. For two tubes normal to flow, five flow velocities are tested: 0.05, 0.07, 0.113, 0.146, and 0.166 m/s. For all other tests, three flow velocities are tested: 0.07, 0.11, and 0.15 m/s. Reynolds number varies from about 1200 to 4200. In all tests, when the flow speed was set at 0.15 m/s, different excitation levels were given to determine the fluid-force coefficients as a function of excitation level.

Fluid-damping and fluid-stiffness coefficients are obtained for both two tubes normal to flow and two tubes in tandem. The following data are available:

Two Tubes Normal to Flow: Fluid-force coefficients due to the motion of tube 1 in the x and y directions.

Two Tubes in Tandem: Fluid-force coefficients due to the motion of tube 1 in the x and y directions and due to the motion of tube 2 in the x and y directions.

To limit the length of this paper, only the data for two tubes normal to flow are presented, Figs. 4-9. Readers who are interested in additional data can contact the authors for additional force coefficients.

Note that Figs. 4-7 show the fluid-force coefficients as a function of reduced flow velocity at several flow velocities while Figs. 8 and 9 show the fluid-force coefficients as a function of excitation level.

From the data, some general characteristics of motion-dependent fluid-force coefficients are noticed:

1. High Reduced Flow Velocity

When the reduced flow velocity is high, say larger than 20 and some larger than 10, all fluid-force coefficients are approximately independent of reduced flow velocity. This shows that when the flow velocity is high in comparison with cylinder velocity, the fluid forces resulting from tube motion can be quantified at a specific velocity and its results can be applied to other flow velocities. In this range, measurements of fluid forces can be significantly reduced. This characteristic is not only valid for circular cylinders, but also valid for other geometries (Chen and Chandra 1991).

2. Reynolds Number

At low reduced flow velocity, fluid-force coefficients depend on the reduced flow velocity, Reynolds number, and excitation amplitude. Similar characteristics have been noticed for a single cylinder (Chen, Zhu, and Cai 1995). This can be seen from the results given in Figs. 4-9. For example, the coefficient for U_r less than 8 are shown in Fig. 10. The peak values decrease with flow velocity and are shifted toward larger U_r. This trend is similar to those of a single tube. At lower reduced flow velocity, fluid-force coefficients are much more complicated.

5. DYNAMIC RESPONSE IN CROSSFLOW

Consider two identical tubes with radius R subjected to crossflow as shown in Fig. 11. The axes of the tube are parallel to the z-axis and flow is parallel to the x-axis. The subscript j is used to denote variables associated with tube j. The variables associate with the motion in the x and y directions are flexural rigidity EI, cylinder mass per unit length m, structural damping coefficient C_s, and displacement u_j and v_j. The equations of motion for tube j in the x and y directions are (Chen 1987)

$$EI\frac{\partial^4 u_j}{\partial z^4}+C_s\frac{\partial u_j}{\partial t}+m\frac{\partial^2 u_j}{\partial t^2}+\sum_{k=1}^{2}\rho\pi R^2\left(\alpha_{jk}\frac{\partial^2 u_k}{\partial t^2}+\sigma_{jk}\frac{\partial^2 v_k}{\partial t^2}\right)$$

$$-\sum_{k=1}^{2}\left(\frac{\rho U^2}{\omega}\alpha'_{jk}\frac{\partial u_k}{\partial t}+\frac{\rho U^2}{\omega}\sigma'_{jk}\frac{\partial v_k}{\partial t}\right)-\sum_{k=1}^{2}\rho U^2\left(\alpha''_{jk}u_k+\sigma''_{jk}v_k\right)=f_j \quad (11)$$

$$EI\frac{\partial^4 v_j}{\partial z^4}+C_s\frac{\partial v_j}{\partial t}+m\frac{\partial^2 v_j}{\partial t^2}+\sum_{k=1}^{2}\rho\pi R^2\left(\tau_{jk}\frac{\partial^2 u_k}{\partial t^2}+\beta_{jk}\frac{\partial^2 v_k}{\partial t^2}\right)$$

$$-\sum_{k=1}^{2}\left(\frac{\rho U^2}{\omega}\tau'_{jk}\frac{\partial u_k}{\partial t}+\frac{\rho U^2}{\omega}\beta'_{jk}\frac{\partial v_k}{\partial t}\right)-\sum_{k=1}^{2}\rho U^2\left(\tau''_{jk}u_k+\beta''_{jk}\right)=g_j, \quad (12)$$

where f_j and g_j are the excitation forces. Note that fluid-damping coefficients and fluid-stiffness coefficients are functions of reduced flow velocity U_r (= U/fD; f is the oscillation frequency of the cylinders in flow).

The in-vacuum variables are mass per unit length m, modal damping ratio ζ_v and natural frequency f_v (= $\omega_v/2\pi$). The values for f_v and ζ_v can be calculated from the equation of motion and appropriate boundary conditions or from tests in vacuum (practically in air). The modal function of the cylinder vibrating in vacuum and in fluid is $\psi(z)$;

$$\frac{1}{\ell}\int_0^1 \psi^2(z)dz = 1 \tag{13}$$

where ℓ is the length of the cylinders. Let

$$\begin{aligned} u_j(z,t) &= a_j(t)\psi(z), \\ v_j(z,t) &= b_j(t)\psi(z), \end{aligned} \tag{14}$$

where $a_j(t)$ and $b_j(t)$ are functions of time only. Calculation of Eqs. (11) and (12) yields

$$\begin{aligned} &\ddot{a}_j + \gamma \sum_{k=1}^{2}\left(\alpha_{jk}\ddot{a}_k + \sigma_{jk}\ddot{b}_k\right) + 2\zeta_v\omega_v\dot{a}_j - \frac{\gamma}{\pi^3}U_v^2\left(\frac{\omega_v^2}{\omega}\right)\sum_{k=1}^{2}\left(\alpha'_{jk}\dot{a}_k + \sigma'_{jk}\dot{b}_k\right) \\ &\quad + \omega_v^2 a_j - \frac{\gamma}{\pi^3}U_v^2\omega_v^2\sum_{k=1}^{2}\left(\alpha''_{jk}a_k + \sigma''_{jk}b_k\right) = p_j \end{aligned} \tag{15}$$

$$\begin{aligned} &\ddot{b}_j + \gamma \sum_{k=1}^{2}\left(\tau_{jk}\ddot{a}_k + \beta_{jk}\ddot{b}_k\right) + 2\zeta_v\omega_v\dot{b}_j - \frac{\gamma}{\pi^3}U_v^2\left(\frac{\omega_v^2}{\omega}\right)\sum_{k=1}^{2}\left(\tau'_{jk}\dot{a}_k + \beta'_{jk}\dot{b}_k\right) \\ &\quad + \omega_v^2 b_j - \frac{\gamma}{\pi^3}U_v^2\omega_v^2\sum_{k=1}^{2}\left(\tau''_{jk}a_k + \beta''_{jk}b_k\right) = q_j, \end{aligned} \tag{16}$$

where the dot denotes differentiation with respect to time and

$$
\begin{aligned}
U_v &= \frac{U}{f_v D}, \\
\gamma &= \frac{\rho \pi R^2}{m}, \\
p_j &= \frac{1}{m\ell}\int_0^\ell f_j \psi(z)dz, \\
q_j &= \frac{1}{m\ell}\int_0^\ell g_j \psi(z)dz.
\end{aligned}
\tag{17}
$$

Constrained Modes

When one the tubes is allowed to oscillate in a specific direction while the other tubes are rigid, the equations of motion can be simplified significantly. For example, tube 1 is oscillating in the x direction, its equation of motion based on Eq. 15 becomes

$$
\frac{d^2 a_{jj}}{dt^2} + 2\zeta\omega \frac{da_{jj}}{dt} + \omega^2 a_{jj} = \frac{p_j}{1+\gamma\alpha_{jj}}, \tag{18}
$$

where

$$
\omega = \omega_v (1+\gamma C_M)^{-0.5},
$$

$$
\zeta = \frac{\zeta_v}{1+\gamma\alpha_{jj}}\left[(1+\gamma C_M)^{0.5} - \frac{\gamma U_r^2 \alpha'_{jj}}{2\zeta_v \pi^3}\right], \tag{19}
$$

$$C_M = \alpha + \frac{U_r^2 \alpha''_{jj}}{\pi^3}.$$

Note that ω and ζ are the circular frequency and modal damping ratio, respectively, for the tube in crossflow. C_M is called an added mass coefficient for the tube in flow; when $U_r = 0$, it is equal to α_{jj}. When U_r is not equal to zero, C_M depends on U_r as well as on α''_{jj}, which in turn, depends on U_r and oscillation amplitude.

From Eqs. 18 it is noted that when α'_{jj} is positive, it will contribute to negative damping to the system. In some cases, the resultant damping may become zero and the system will become unstable. From Eq. 19 the critical reduced flow velocity at which the modal damping ratio is zero can be calculated from

$$U_r = 4\sqrt{2\pi}\left(\frac{\delta}{\alpha'_{jj}}\right)^{0.5}\left[\frac{\delta}{\pi^2}\left(\frac{\alpha''_{jj}}{\alpha'_{jj}}\right) \pm \sqrt{\left(\frac{\delta}{\pi^3}\right)^2 + \frac{1+\gamma\alpha_{jj}}{4}}\right]^{0.5}, \tag{20}$$

where δ is a mass-damping parameter ($\delta = 2\pi\zeta_v m/\rho D^2$). This is the critical flow velocity for fluidelastic instability.

Equations 18-20 can also be applied to oscillations in the y direction. Replacing all α by β in Eqs. 18-20 yields the equations of motion and stability criterion for constrained mode in the y direction. From Eqs. 19 and 20, it is noted that when the value of the fluid damping coefficient, α'_{jj} or β'_{jj}, is positive, the tube may become unstable. The region depends on tube arrangement, location, and flow velocity. From the fluid-force coefficients, α'_{jj} is found to be positive in the regions given in Table 1.

Table 1. Regions of reduced flow velocity in which fluid-damping coefficients, α'_{11} and α'_{22}, are positive

	Flow Velocity (m/s)	Reduced Flow Velocity
Two Tubes Normal to Flow		
α'_{11} or α'_{22}	0.05	1.7 to 4.3
	0.07	1.8 to 4.7
	>0.13	2.3 to 5.6
Two Tubes in Tandem		
α'_{11}	0.07	>6.0
	0.11	>7.1
	0.15	>7.4
α'_{22}	0.07	>3.2
	0.11	>3.6
	0.15	>3.6

Fluid-damping coefficients in the y direction β'_{11} and β'_{22} are always negative; this means that oscillation in the y direction will not become unstable.

The natural frequencies of constrained modes are affected by α''_{jj} and β''_{jj}. When the fluid-stiffness coefficient is positive, the frequency is reduced. The regions in which α''_{11} and α''_{22} are positive are given in Table 2.

Table 2. Regions of reduced flow velocity in which fluid-stiffness coefficients, α''_{11} and α''_{22}, are positive

	Flow Velocity (m/s)	Reduced Flow Velocity
Two Tubes Normal to Flow		
α''_{11} or α''_{22}	0.05	<1.7
	0.07	<2.1
	0.113	<2.5
	0.146	<3.2
	0.166	<3.4
Two Tubes in Tandem		
α''_{11}	0.07	>12.5
	0.11	>14.0
	0.15	>15.8
α''_{22}	0.07	>1.8
	0.11	>2.2
	0.15	>5.2

Fluid-stiffness for oscillations in the y direction, β''_{jj} is negative for two tubes normal to flow and the upstream tube. The downstream tube β''_{22} becomes positive when U_r is larger than 8.2.

Coupled Vibration

In flowing fluid, from Eqs. 15 and 16 the natural frequencies and modal damping ratios of the system can be calculated as follows:

$$f = f(\gamma,\zeta_v,U_v),$$
$$\zeta = \zeta(\gamma,\zeta_v,U_v). \tag{21}$$

It should be noted that fluid-damping and fluid-stiffness coefficients are functions of U_r (= U/fD); therefore, a numerical method is needed to calculate f and ζ.

The stability of a cylinder array is determined from equations (15) and (16). The nondimensional parameters in equations (15) and (16) are γ, ζ_v, U_v, α_{jk}, σ_{jk}, τ_{jk}, β_{jk}, α'_{jk}, σ'_{jk}, τ'_{jk}, β'_{jk}, α''_{jk}, σ''_{jk}, τ''_{jk}, and β''_{jk}. Therefore, the critical flow velocity can be written in a functional form as

$$U_v = F(\gamma,\zeta_v,\omega_v/\omega,\ \alpha_{jk},\sigma_{jk},\tau_{jk},\beta_{jk},\alpha'_{jk},\sigma'_{jk},\tau'_{jk},\beta'_{jk},\alpha''_{jk},\sigma''_{jk},\tau''_{jk},\beta''_{jk}). \tag{22}$$

For two tubes, if fluid-force coefficients are independent of U_r, then

$$U_v = F(\gamma,\zeta_v),$$

or,

$$U_r = \frac{f_v}{f}F(\gamma,\zeta_v), \tag{23}$$

i.e., the critical flow velocity is a function of mass ratio and damping ratio only.

Fluidelastic Instability in Light Fluid

In a light fluid, fluid inertia and damping associated with the quiescent fluid can be neglected. Equations (15) and (16) can be written

$$\ddot{a}_j + 2\zeta_v\omega_v\dot{a}_j + \omega_v^2 a_j - \frac{\gamma}{\pi^3}U_v^2\sum_{k=1}^{2}\left[\frac{\omega_v^2}{\omega}\left(\alpha'_{jk}\dot{a}_{jk} + \sigma'_{jk}b_k\right) + \omega_v^2\left(\alpha''_{jk}a_k + \sigma''_{jk}b_k\right)\right] = p_j,$$

$$\ddot{b}_j + 2\zeta_v\omega_v\dot{b}_j + \omega_v^2 b_j - \frac{\gamma}{\pi^3}U_v^2\sum_{k=1}^{2}\left[\frac{\omega_v^2}{\omega}\left(\tau'_{jk}\dot{a}_{jk} + \beta'_{jk}b_k\right) + \omega_v^2\left(\tau''_{jk}a_k + \beta''_{jk}b_k\right)\right] = q_j. \tag{24}$$

In a light fluid, all fluid-force coefficients are approximately independent of U_r and the oscillation frequency is approximately equal to ω_v (i.e., $\omega_v = \omega_f$). Then γU_v^2 plays the same role as ζ_v; both of them contribute to system damping. The modal damping for a particular mode can be written

$$\zeta = \zeta_v - C\,\gamma U_v^2 \tag{25}$$

where C depends on fluid-damping and fluid-stiffness coefficients. Instability occurs if $\zeta = 0$; i.e.,

$$U_v = \frac{1}{C}\left(\frac{\zeta_v}{\gamma}\right)^{0.5} \tag{26}$$

or

$$\frac{U}{f_v D} \propto \left(\frac{2\pi\zeta_v m}{\rho D^2}\right)^{0.5}. \tag{27}$$

Thus, the critical flow velocity is a function of the mass-damping parameter and proportional to its half-power.

CLOSING REMARKS

In the past, the motion-dependent fluid forces for two tubes were not quantified in general. In this study, fluid-damping and fluid-stiffness coefficients for two tubes normal to flow and two tubes in tandem with the pitch-to-diameter ratio of 1.35 are presented as a function of reduced flow velocity for a series of Reynolds number. At high reduced flow velocity, the fluid-force coefficients are practically independent of reduced flow velocity. However, at low reduced flow velocity, fluid-damping and fluid-stiffness coefficients depend on reduced flow velocity, Reynolds number, and oscillation amplitude.

Once fluid damping and fluid stiffness are known, the response of two tubes in crossflow can be predicted on the basis of the unsteady flow theory. Fluid damping and fluid stiffness play an important role in determining tube response. The system may become unstable due to motion-dependent fluid forces. For example, fluid-damping-controlled instability can occur even in constrained mode.

Various approximate theories for two tubes in crossflow are useful in specific conditions. The unsteady flow theory accounts for the interaction of tube motions and flow field adequately; it can be applied to various conditions. The key elements of the unsteady flow theory are the motion-dependent fluid forces. It requires an extensive effort to obtain these forces experimentally. Some studies have been published to calculate these forces numerically (Sadaoka and Umegaki 1993, Ichioka et al. 1994). It is expected that once it is developed, computation fluid dynamics method will be more economic.

ACKNOWLEDGMENTS

This work was jointly funded by the U. S. Department of Energy, Office of Basic Energy Sciences, Division of Engineering and Geosciences, under Contract W-31-109-Eng-38, and by Taiwan Power Company under an agreement with the U. S. Department of Energy, Contract Agreement 31-109-Eng-38-85847.

REFERENCES

Chen, S. S. 1975. "Vibration of Nuclear Fuel Bundles." Nuclear Engineering and Design, Vol. 35, pp. 399-422.

Chen, S. S. 1986. "A Review of Flow-Induced Vibration of Two Circular Cylinders in Crossflow." Journal of Pressure Vessel Technology, Vol. 108, pp. 382-393.

Chen, S. S. 1987. "Flow-Induced Vibration of Circular Cylindrical Structures." Hemisphere Publishing Corporation, New York.

Chen, S. S., and Chandra, S. 1991. "Fluidelastic Instabilities in Tube Bundles Exposed to Nonuniform Cross-Flow," Journal of Fluids and Structures, Vol. 5, pp. 299-322.

Chen, S. S., and Jendrzejczyk, J. A. 1978. "Experiments on Fluidelastic Vibration of Cantilevered Tube Bundles." Journal of Mechanical Design, Vol. 110, pp. 540-548.

Chen, S. S., Zhu, S., and Cai, Y. 1995. "An Unsteady Flow Theory for Vortex Induced Vibration." Journal of Sound and Vibration, in press.

Ichioka, T., Kawata, Y., and Izumi, H. 1994. "Two-Dimensional Flow Analysis of Fluid Structure Interaction Around a Cylinder and a Row of Cylinders." ASME Publication, PVP-Vol. 273, pp. 33-41.

Sadaoka, N., and Umegaki, K. 1993. "A Numerical Method to Calculate Flow-Induced Vibrations in a Turbulent Flow." ASME Publication, PVP-Vol. 258, pp. 83-94.

Zdravkovich, M. M. 1977. "Review of Flow Interference between Two Circular Cylinders in Various Arrangements." Journal of Fluids Engineering, Vol. 99, pp. 618-633.

Figure Captions

1 Two tubes in crossflow

2 Motion-dependent fluid forces (Fig. 2a, 2b, 2c, and 2d) acting on the two tubes with the pitch-to-diameter ratio of 1.35 (Fig. 1a) due to motion u_1 (Fig. 2e)

3a Added mass coefficidnts, α_{11} and α_{21}, and fluid-damping coefficients, $\overline{\alpha}'_{11}$ and $\overline{\alpha}'_{21}$

3b Added mass coefficients, τ_{11} and τ_{21}, and fluid-damping coefficients, $\overline{\tau}'_{11}$ and $\overline{\tau}'_{21}$

4 Fluid-damping and fluid-stiffness coefficients, α'_{11}, τ'_{11}, α''_{11}, and τ''_{11} for two tubes normal to flow

5 Fluid-damping and fluid-stiffness coefficients, α'_{21}, τ'_{21}, α''_{21}, and τ''_{21} for two tubes normal to flow

6 Fluid-damping and fluid-stiffness coefficients, β'_{11}, σ'_{11}, β''_{11}, and σ''_{11} for two tubes normal to flow

7 Fluid-damping and fluid-stiffness coefficients, β'_{21}, σ'_{21}, β''_{21}, and σ''_{21} for two tubes normal to flow

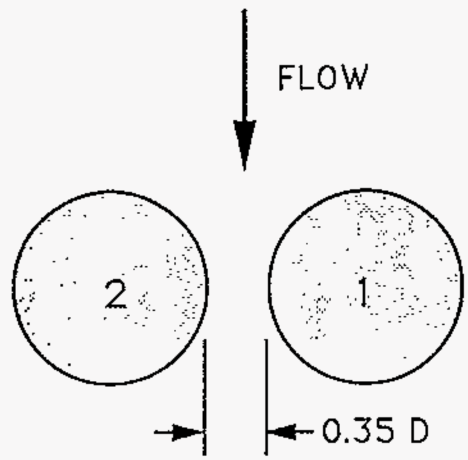

(a) TWO TUBES NORMAL TO FLOW

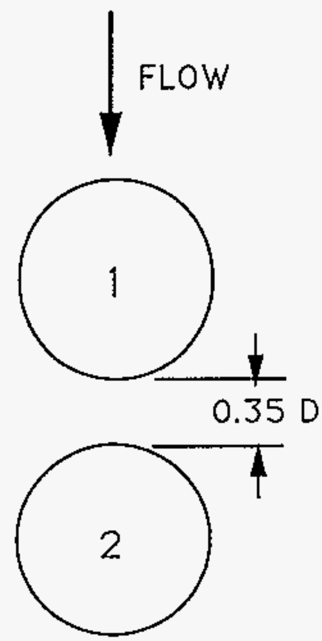

(b) TWO TUBES IN TANDEM

Fig. 1

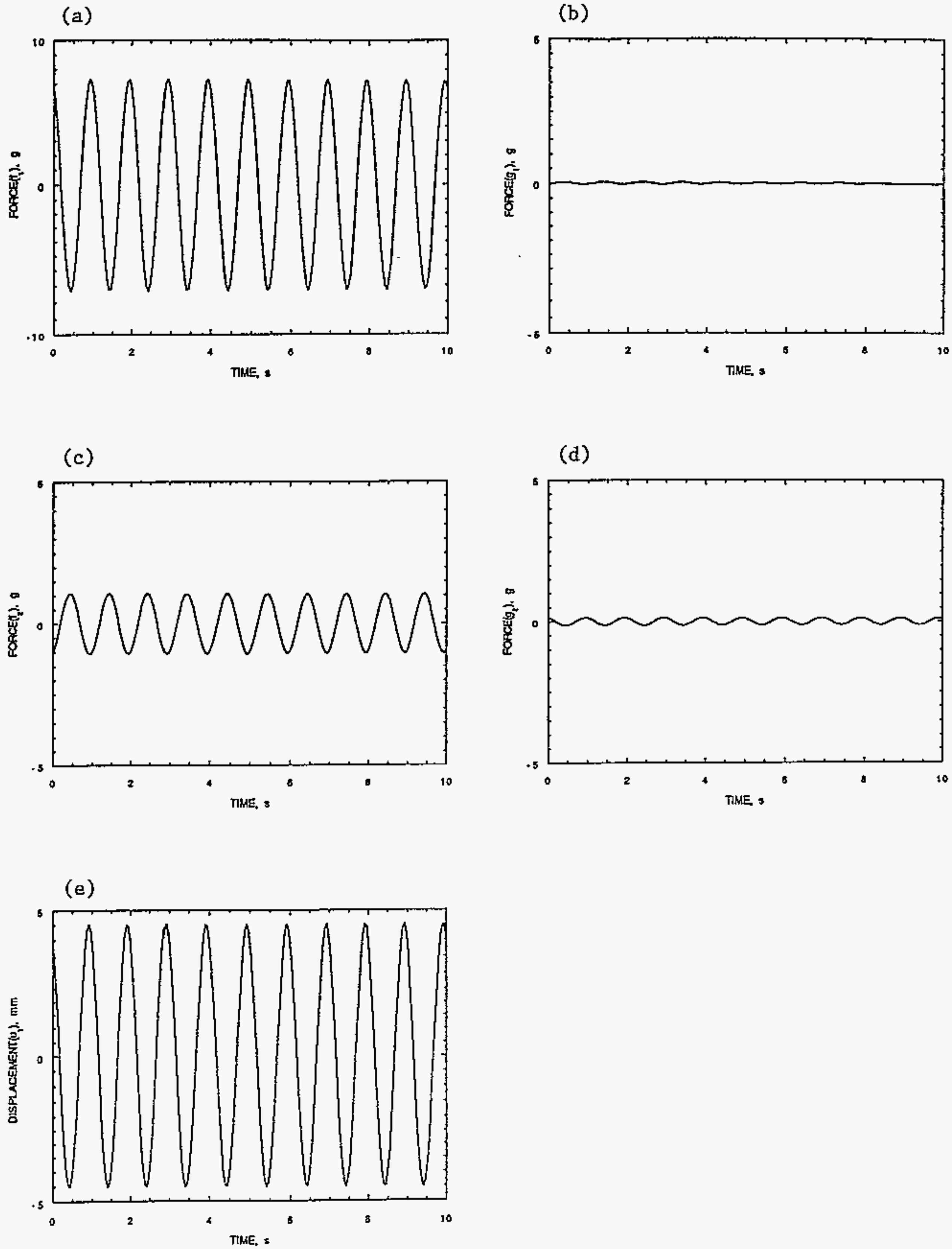
(a)
FORCE(f_1), g
TIME, s
(b)
FORCE(g_1), g
TIME, s
(c)
FORCE(f_2), g
TIME, s
(d)
FORCE(g_2), g
TIME, s
(e)
DISPLACEMENT(u_1), mm
TIME, s

F.g. 5

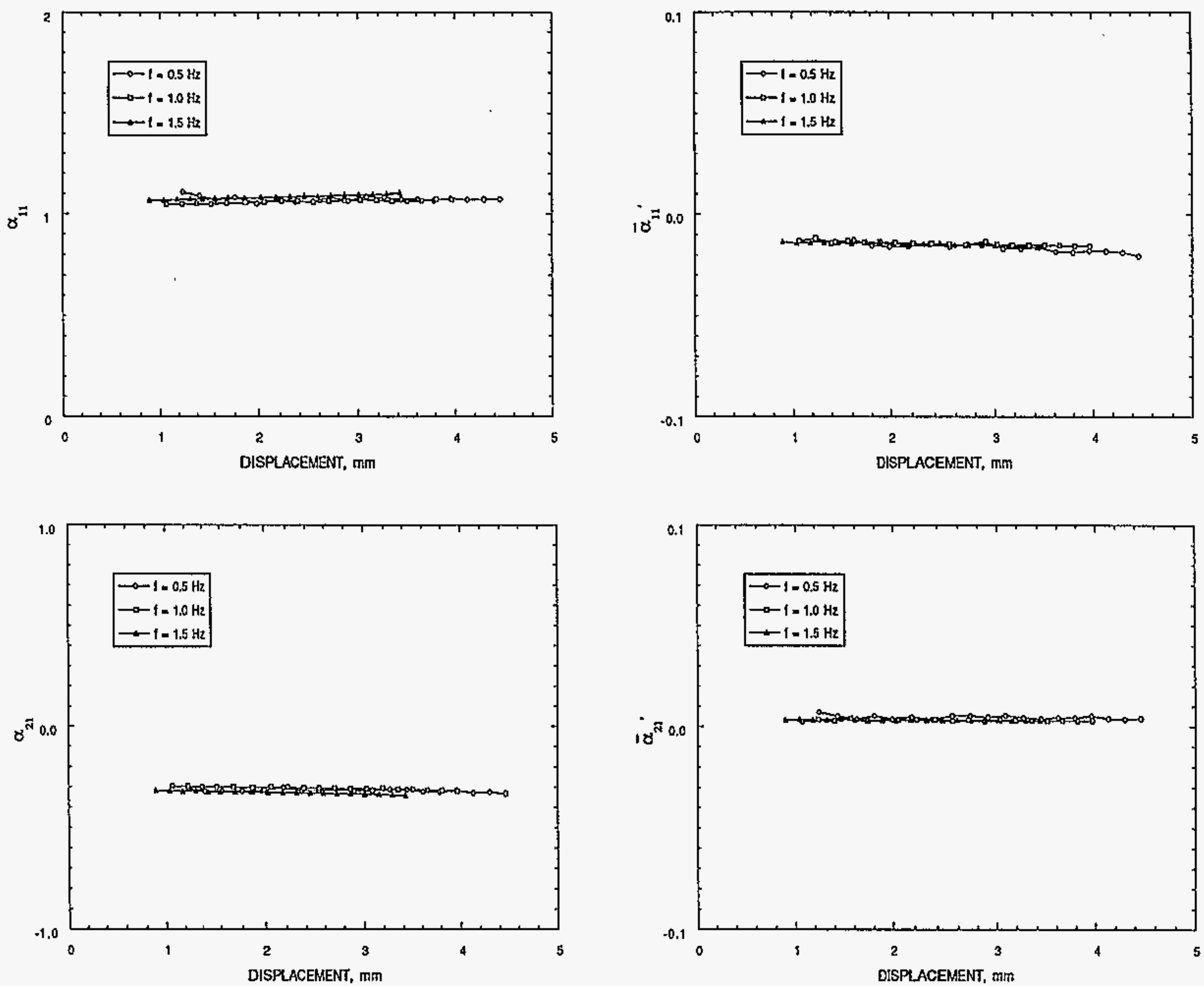

f = 0.5 Hz
f = 1.0 Hz
f = 1.5 Hz
α_{11}
DISPLACEMENT, mm
$\bar{\alpha}_{11}'$
α_{21}
$\bar{\alpha}_{21}'$

Fig 3a

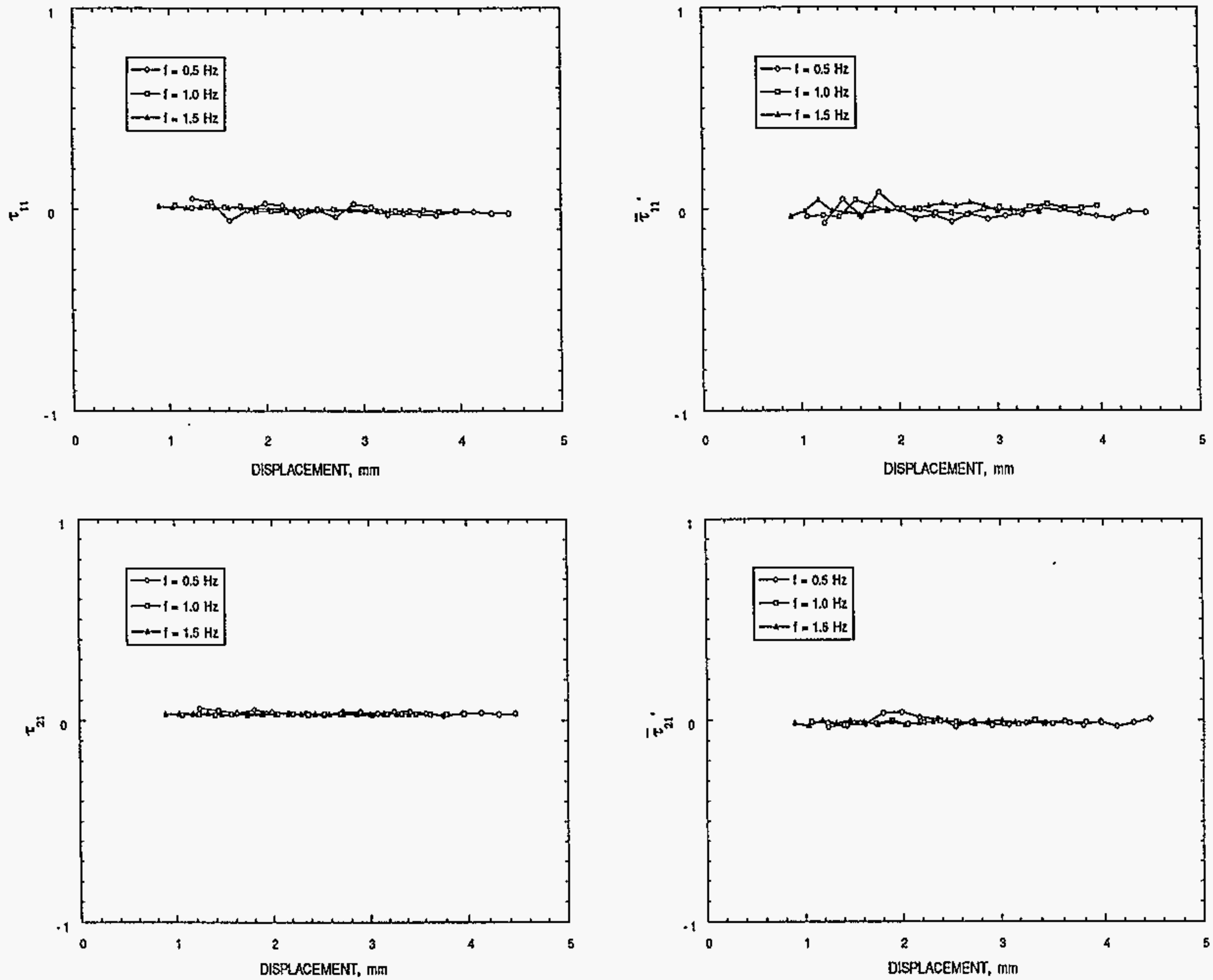

f = 0.5 Hz
f = 1.0 Hz
f = 1.5 Hz
τ_{11}
$\bar{\tau}_{11}'$
τ_{21}
$\bar{\tau}_{21}'$
DISPLACEMENT, mm

Fig 3b

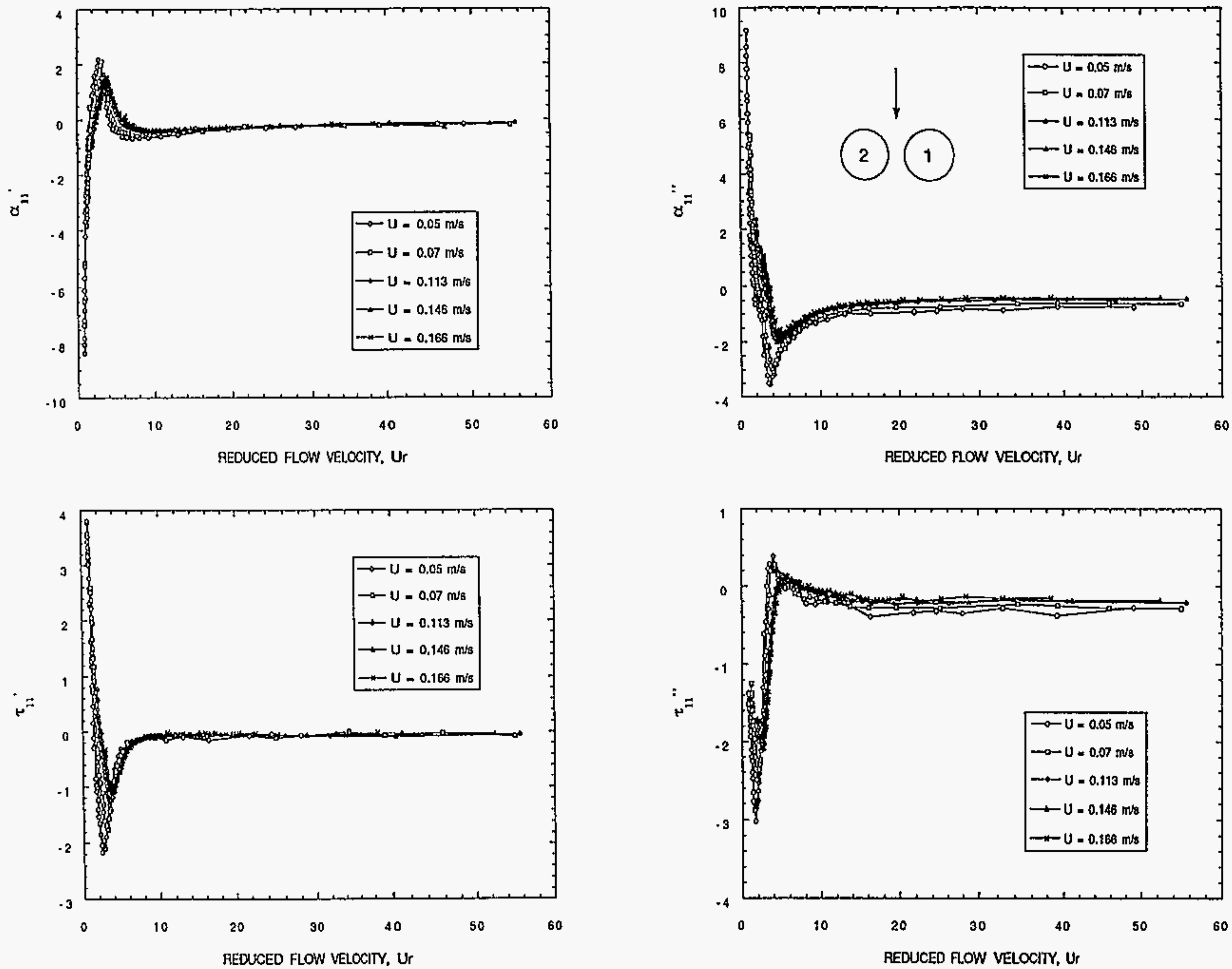

α_{11}'
α_{11}''
τ_{11}'
τ_{11}''
REDUCED FLOW VELOCITY, Ur
U = 0.05 m/s
U = 0.07 m/s
U = 0.113 m/s
U = 0.146 m/s
U = 0.166 m/s
2
1

Fig. 4

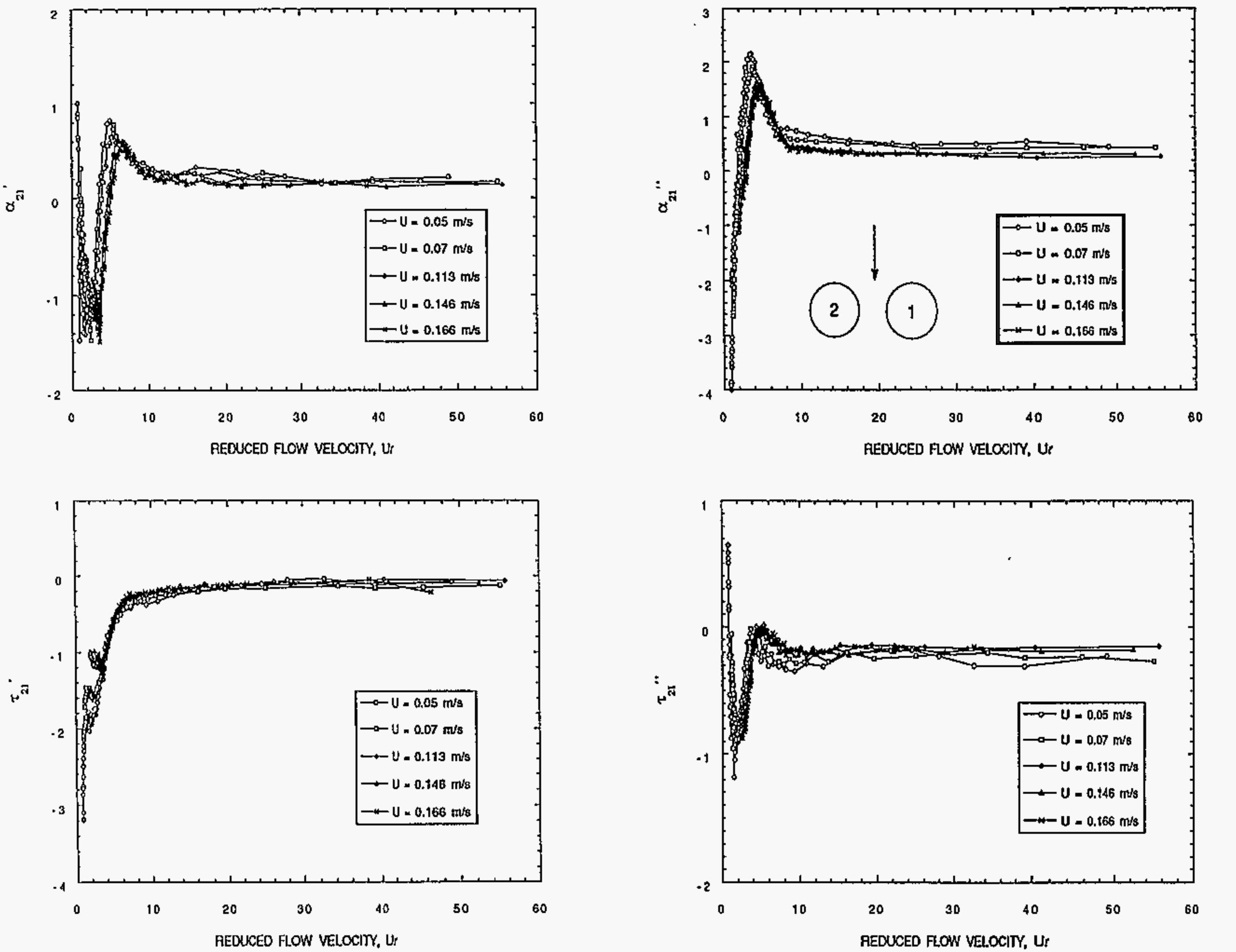

α_{21}'
α_{21}''
τ_{21}'
τ_{21}''
REDUCED FLOW VELOCITY, Ur
U = 0.05 m/s
U = 0.07 m/s
U = 0.113 m/s
U = 0.146 m/s
U = 0.166 m/s
2
1

Fig. 5

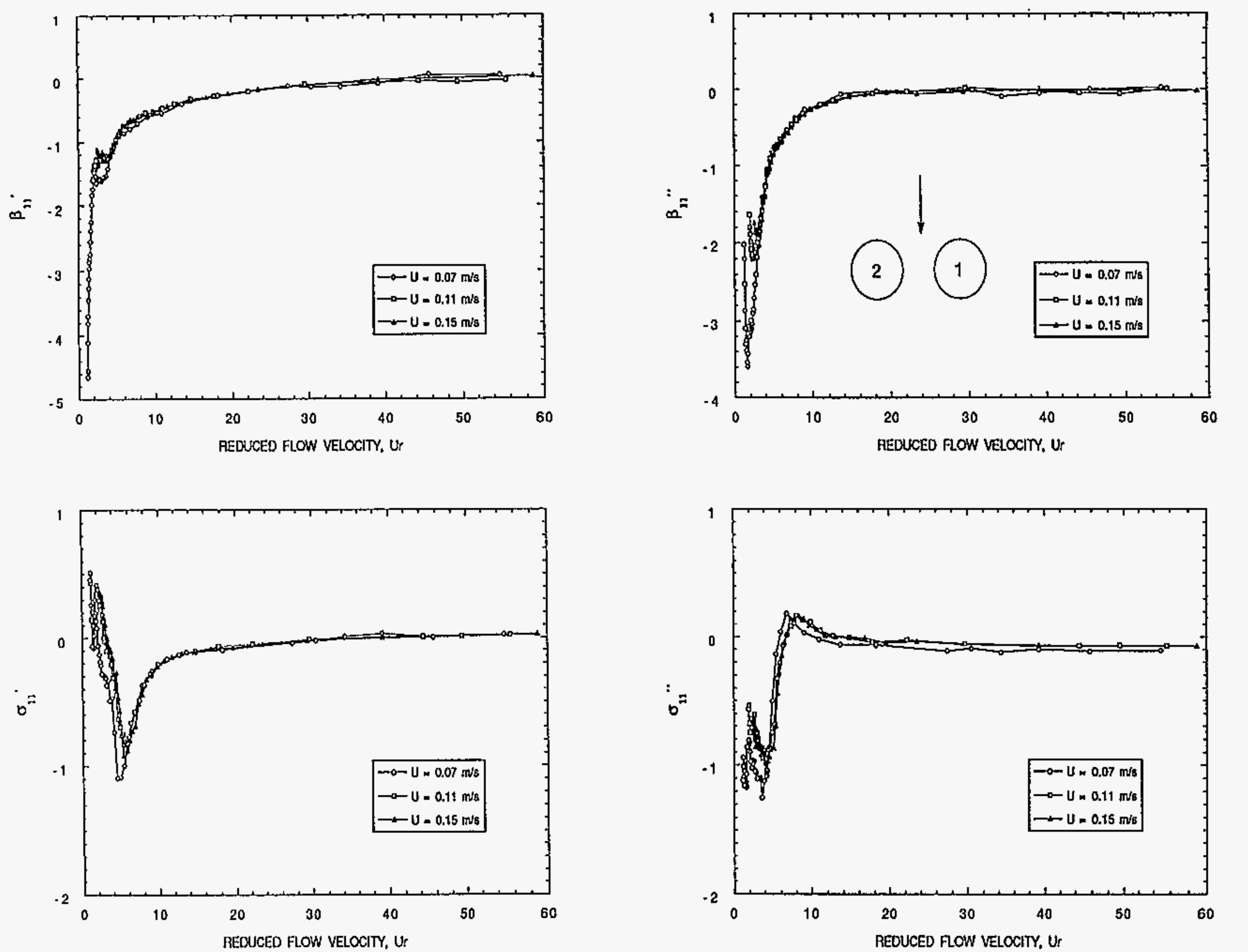
β11'
β11''
σ11'
σ11''
REDUCED FLOW VELOCITY, Ur
U = 0.07 m/s
U = 0.11 m/s
U = 0.15 m/s
1
2

Fig. 6

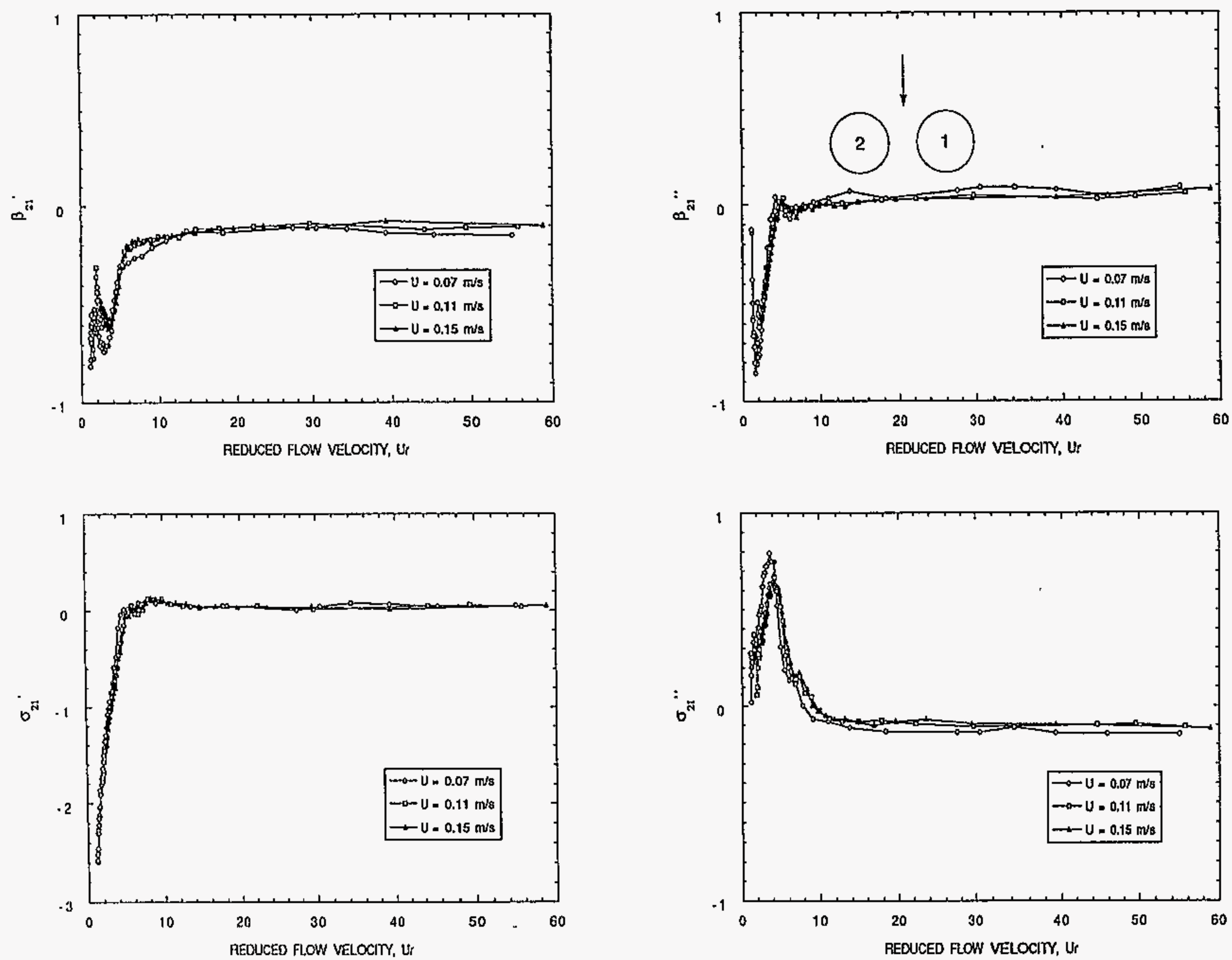
β21'
U = 0.07 m/s
U = 0.11 m/s
U = 0.15 m/s
REDUCED FLOW VELOCITY, Ur
β21''
2
1
σ21'
σ21''

Fig 7

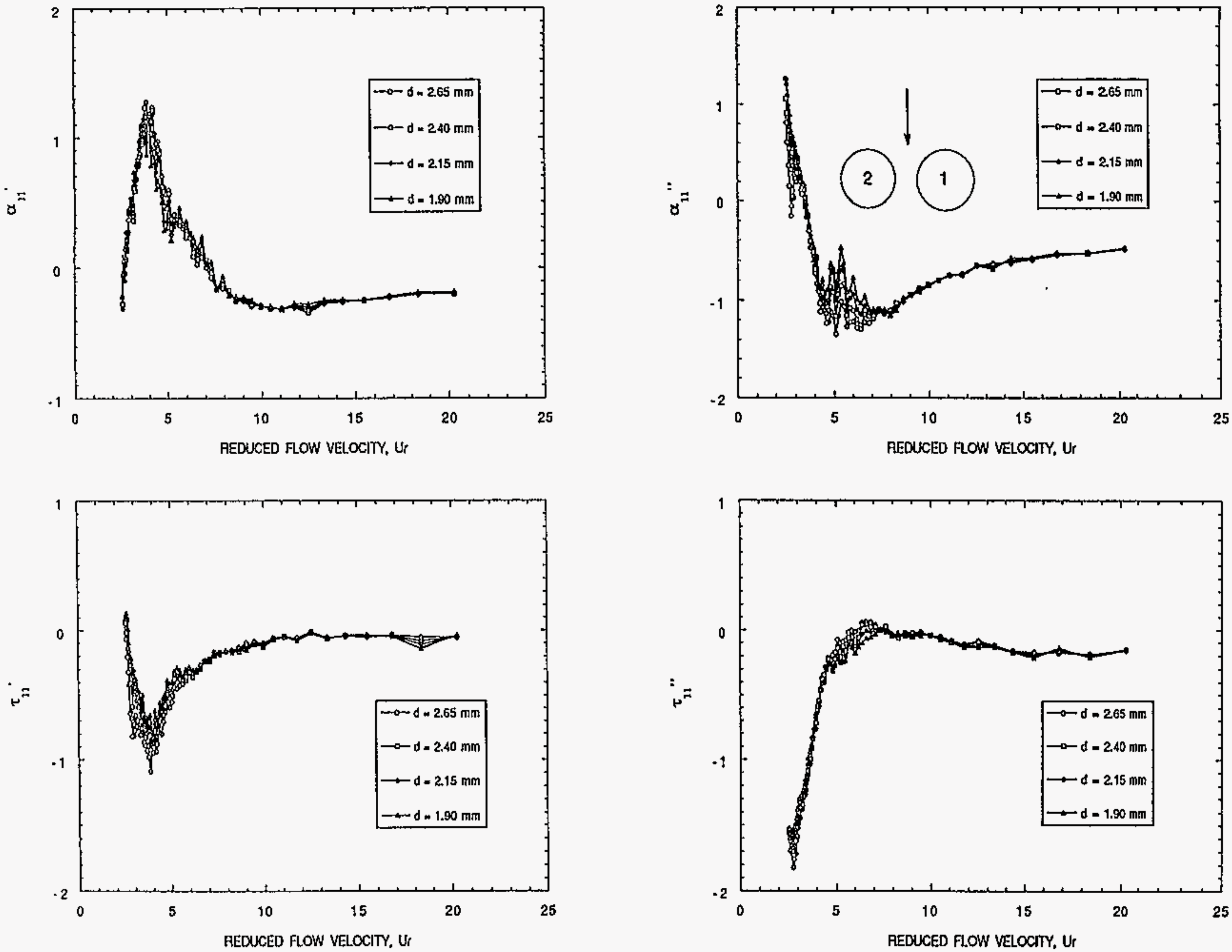

Fig. 8

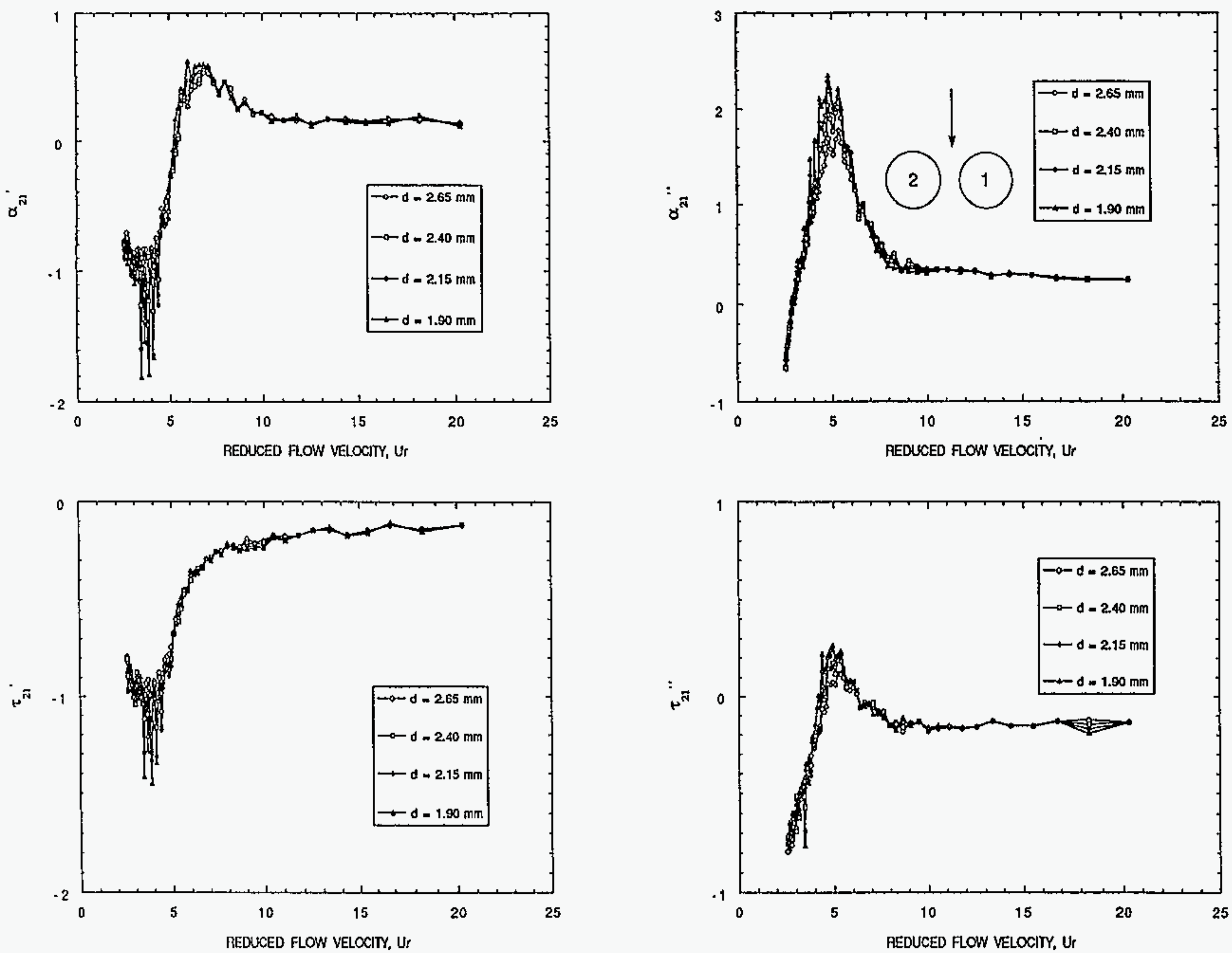

α_{21}'
α_{21}''
τ_{21}'
τ_{21}''
REDUCED FLOW VELOCITY, Ur
d = 2.65 mm
d = 2.40 mm
d = 2.15 mm
d = 1.90 mm
2
1

Fig 9

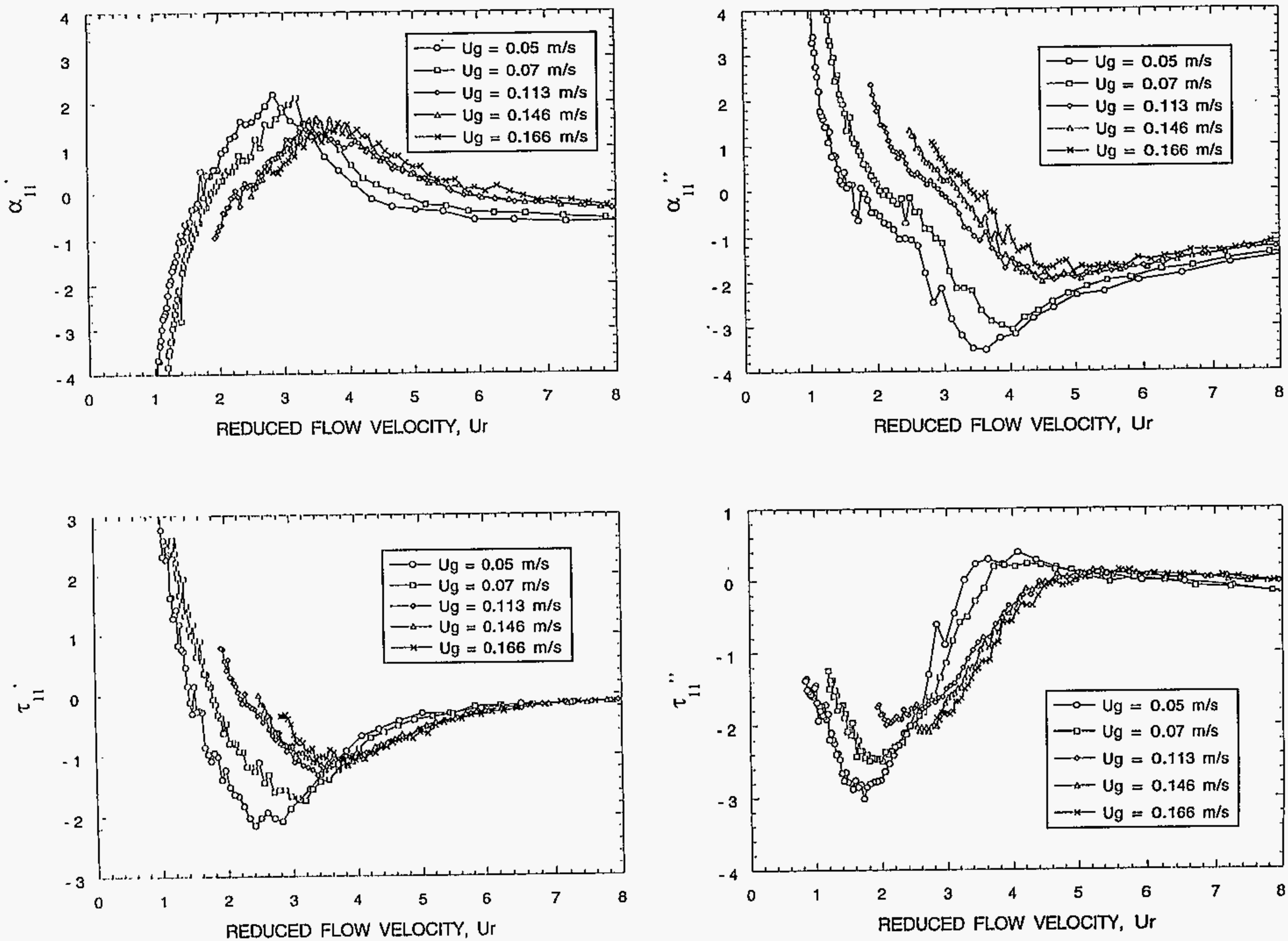
Ug = 0.05 m/s
Ug = 0.07 m/s
Ug = 0.113 m/s
Ug = 0.146 m/s
Ug = 0.166 m/s
REDUCED FLOW VELOCITY, Ur
α'_{11}
α''_{11}
τ'_{11}
τ''_{11}

Fig. 10

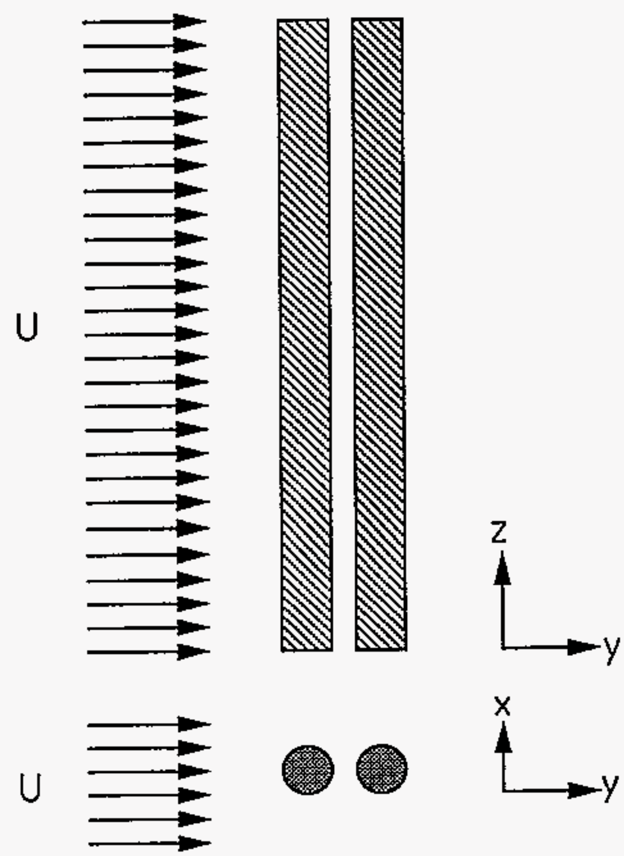

Fig. 11